J|A|C|S
ARTICLES
Published on Web 12/17/2005

Gauging the Relative Oxidative Powers of Compound I, Ferric-Hydroperoxide, and the Ferric-Hydrogen Peroxide Species of Cytochrome P450 Toward C−H Hydroxylation of a Radical Clock Substrate

Etienne Derat, Devesh Kumar, Hajime Hirao, and Sason Shaik*

Contribution from the Department of Organic Chemistry and the Lise Meitner-Minerva Center for Computational Quantum Chemistry, The Hebrew University of Jerusalem, 91904 Jerusalem, Israel

Received September 14, 2005; E-mail: sason@yfaat.ch.huji.ac.il

Abstract: Density functional calculations were performed in response to the controversies regarding the identity of the oxidant species in cytochrome P450. The calculations were used to gauge the relative C−H hydroxylation reactivity of three potential oxidant species of the enzyme, the high-valent oxo-iron species Compound I (Cpd I), the ferric hydroperoxide Compound 0 (Cpd 0), and the ferric-hydrogen peroxide complex Fe(H_2O_2). The results for the hydroxylation of a radical probe substrate, **1**, show the following trends: (a) Cpd I is the most reactive species; in its presence the other two reagents will be silent. (b) In the absence of Cpd I, substrate oxidation by Cpd 0 and Fe(H_2O_2) will take place via a stepwise mechanism that involves initial O−O homolysis followed by H-abstraction from **1**. (c) Cpd 0 will undergo mostly porphyrin hydroxylation and only ∼15% of substrate oxidation producing mostly the rearranged alcohol, **3** (Scheme 2). (d) Fe(H_2O_2) will generate mostly free hydrogen peroxide (uncoupling). A small fraction will perform substrate oxidation and lead mostly to **3**. Reactivity probes for these reagents are kinetic isotope effect (KIE) and the product ratio of unrearranged to rearranged alcohols, [**2**/**3**]. Thus, for substrate oxidation by Cpd 0 or Fe(H_2O_2) KIE will be small, ∼2, while Cpd I will have large KIE values. Typically both Cpd 0 and Fe(H_2O_2) will lead to a [**2**/**3**] ratio < 1, while Cpd I will lead to ratios > 1. In addition, the product isotope effect ($KIE_2/KIE_3 \neq 1$) is expected from the reactivity of Cpd I.

Introduction

The identity of the oxidant species of the enzymes cytochromes P450 is still elusive.[1,2] There is a consensus[1,2] that the primary oxidant is the high-valent oxo-ferryl species, so-called Compound I (Cpd I),[3] which is generated from the precursor species ferric-hydroperoxide, so-called Compound 0 (Cpd 0), in Scheme 1. Spectroscopic data of $P450_{cam}$ (CYP101) and the thermophilic P450 enzyme (CYP119) treated with oxygen donor reagents[4] revealed a transient electronic-absorption signature typical of Cpd I species of the analogous thiolate enzyme, chloroperoxidase.[5] Other attempts to characterize Cpd I by EPR and Mössbauer spectroscopies led to the formation of the reduced species of Cpd I (sometimes called Compound II, Cpd II) and a protein radical.[6]

Cryogenic EPR/ENDOR spectroscopy of $P450_{cam}$ provided indirect evidence that Cpd I is responsible for camphor hydroxylation.[7] Nevertheless, the last observable species in the cycle was the ferric-hydroperoxide species, Cpd 0 in Scheme 1. Recent kinetic isotope effect (KIE) measurements with $P450_{cam}$ and $P450_{2E1}$, using substituted *N*,*N*-dimethylaniline *N*-oxide derivatives serving both as oxygen atom donors to P450s and as oxidizable *N*,*N*-dimethylaniline substrates, led to the same KIE values determined from the normal oxidation of the *N*,*N*-dimethylaniline substrates by the NAD(P)H/NAD(P)-reductase-O_2 process of P450s.[8] This equality of the two sets of KIE data demonstrated that Cpd I is the most reasonable oxidant in both systems.[8] Other results show that the product distribution and stereochemical scrambling for a few substrates obtained during P450 oxidation are reproduced using synthetic Cpd I species.[9]

(1) Ortiz de Montellano, P. R., Ed., *Cytochrome P450: Structure, Mechanisms and Biochemistry*, 3rd ed.; Kluwer Academic/Plenum Press: New York, 2005.
(2) Denisov, I. G.; Makris, T. M.; Sligar, S. G.; Schlichting, I. *Chem. Rev.* **2005**, *105*, 2253−2278.
(3) Harris, D. *Curr. Opin. Chem. Biol.* **2001**, *5*, 724−735.
(4) (a) Egawa, T.; Shimada, H.; Ishimura, Y. *Biochem. Biophys. Res. Commun.* **1994**, *201*, 1464−1469. (b) Kellner, D. G.; Hung, S.-C.; Weiss, K. E.; Sligar, S. G. *J. Biol. Chem.* **2002**, *277*, 9641−9644.
(5) (a) Harris, D.; Loew, G.; Waskell, L. *J. Inorg. Biochem.* **2001**, *83*, 309−318. (b) Egawa, T.; Proshlyakov, D. A.; Miki, H.; Makino, R.; Ogura, T.; Kitagawa, T.; Ishimura, Y. *J. Biol. Inorg. Chem.* **2001**, *6*, 46−54. (c) Hager, L. P.; Doubek, D. L.; Silverstein, R. M.; Hargis, J. H.; Martin, J. C. *J. Am. Chem. Soc.* **1972**, *94*, 4364−4366.
(6) (a) Schunemann, V.; Jung, C.; Trautwein, A. X.; Mandon, D.; Weiss, R. *FEBS Lett.* **2000**, *479*, 149−154. (b) Schunemann, V.; Lendzian, F.; Jung, C.; Contzen, J.; Barra, A.-L.; Sligar, S. G.; Trautwein, A. X. *J. Biol. Chem.* **2004**, *279*, 10919−10930. (c) Schunemann, V.; Jung, C.; Terner, J.; Trautwein, A. X.; Weiss, R. *J. Inorg. Biochem.* **2002**, *91*, 586−596.
(7) Davydov, R.; Makris, T. M.; Kofman, V.; Werst, D. E.; Sligar, S. G.; Hoffman, B. M. *J. Am. Chem. Soc.* **2001**, *123*, 1403−1415.
(8) Dowers, T. S.; Rock, D. A.; Jones, J. P. *J. Am. Chem. Soc.* **2004**, *126*, 8868−8869.
(9) Groves, J. T. in *Models and mechanisms of Cytochrome P450 action* in ref 1, Chapter 1, p 1.

Scheme 1. Compound I (Cpd I), Compound 0 (Cpd 0), and Ferric−Hydrogen Peroxide ($Fe(H_2O_2)$) Species of P450 Enzymes

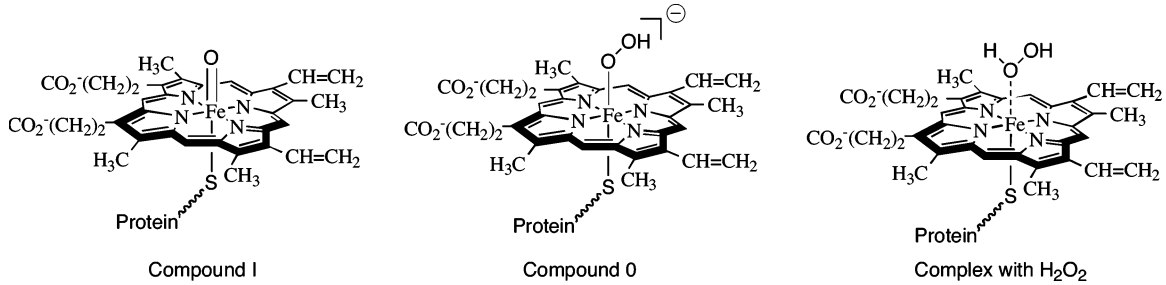

Compound I Compound 0 Complex with H_2O_2

While the chase after Cpd I continues, indirect evidence exists also for the oxidative activity of other species in the cycle.[10] Most of the evidence has been focused on Cpd 0 (Scheme 1), which is the last species seen in the catalytic cycle before the oxidized substrate appears.[7] Especially strong seems the evidence obtained with the T252A mutants of $P450_{cam}$. Thus, the mutation of Thr_{252} to Ala is known to slow or suppress the formation of Cpd I, insofar as the mutant T252A $P450_{cam}$ does not hydroxylate camphor or does so with a very little yield.[2,11] Since the mutant enzyme shows activity toward double bond epoxidation of, e.g., camphene,[10d] this was taken as evidence for the participation of Cpd 0 in epoxidation, even though recent interpretation of the experiment could not rule out the involvement of Cpd I also in this process.[12] This situation has created a tantalizing problem for both experiment and theory: How can one account for the various reactivity patterns of P450?

Density functional calculations by two groups showed that Cpd 0 is not a good electrophile toward ethylene epoxidation,[13] and sulfur oxidation.[14] Nevertheless, ferric-hydrogen peroxide or alkyl peroxide complexes are known to react in heme and nonheme systems.[15] Furthermore, our own group[16] showed recently that Cpd 0 undergoes facile O−O bond homolysis and generates a bound OH• radical, which then performs hydroxylation of the *meso* position of the porphyrin, in a manner analogous to the reaction of heme-oxygenase (HO) enzymes.[17] One may logically surmise that this bound radical can participate also in substrate oxidation in competition with the autoxidation of the porphyrin. Indeed, heme complexes of alkyl peroxides and/or peracids have been amply diagnosed to undergo oxidative reactivity following homolytic O−O cleavage in competition with heterolytic cleavage that leads to Cpd I.[18] These results require a theoretical reassessment of the reactivity of Cpd 0 in the oxidative chemistry of P450, via a homolytic cleavage mechanism, which was recently proposed based on the theoretical investigation of this mechanism in HO.[16] The homolytic mechanism has also experimental precedence in peroxide dependent hydroxylation by P450 isozymes.[18a] This is the first focal point of the present paper.

Recently, the hydrogen peroxide complex, $Fe(H_2O_2)$ in Scheme 1, was also implicated as a possible oxidant, by itself or as a variant of Cpd 0 involving acid catalysis.[19] In fact, there is ample evidence for the presence of free hydrogen peroxide in P450 enzymes;[2] H_2O_2 is considered to be an *uncoupling product* arising from the protonation of the proximal oxygen of Cpd 0, with simultaneous dissociation of the H_2O_2 molecule.[2] While there is no experimental evidence for the existence of a ferric−H_2O_2 complex, as such, in P450, the complex was characterized by DFT calculations and it appears to be a genuine minimum species.[20] A recent Car−Parinello molecular dynamic study confirmed that iron ions and hydrogen peroxide lead to Fenton chemistry.[21,22] Indeed, ferric complexes are generally known to activate hydrogen peroxide,[9,18a,c] and the possibility of oxidative reactivity via an O−O bond homolysis pathway,[16] similar to Cpd 0, may also be viable for the $Fe(H_2O_2)$ complex. Thus, a more general goal of the paper is to gauge the oxidative reactivity of the ferric-hydrogen peroxide complex of P450 compared with Cpd I and Cpd 0.

(10) (a) Vaz, A. D. N.; Pernecky, S. J.; Raner, G. M.; Coon, M. J. *Proc. Natl. Acad. Sci. U.S.A.* **1996**, *93*, 4644−4648. (b) Newcomb, M.; Aebisher, D.; Shen, R.; Chandrasena, R. E. P.; Hollenberg, P. F.; Coon, M. J.; *J. Am. Chem. Soc.* **2003**, *125*, 6064−6065. (c) Volz, T. J.; Rock, D. A.; Jones, J. P. *J. Am. Chem. Soc.* **2002**, *124*, 9724−9725. (d) Jin, S.; Makris, T. M.; Bryson, T. A.; Sligar, S. G.; Dawson, J. H. *J. Am. Chem. Soc.* **2003**, *125*, 3406−3407.

(11) (a) Raag, R.; Martinis, S. A.; Sligar, S. G.; Poulos, T. L. *Biochemistry* **1991**, *30*, 11420−11429. (b) Vidakovic, M.; Sligar, S. G.; Li, H.; Poulos, T. L. *Biochemistry* **1998**, *37*, 9211−9219.

(12) Davydov, R.; Perera, R.; Jin, S.; Yang, T.-C.; Bryson, T. A.; Sono, M.; Dawson, J. H.; Hoffman, B. M. *J. Am. Chem. Soc.* **2005**, *127*, 1403−1413.

(13) (a) Ogliaro, F.; de Visser, S. P.; Cohen, S.; Sharma, P. K.; Shaik, S. *J. Am. Chem. Soc.* **2002**, *124*, 2806−2817. (b) Yoshizawa, K.; Shiota, Y.; Kagawa, Y. *Bull. Chem. Soc. Jpn.* **2000**, *73*, 2669−2673.

(14) Sharma, P. K.; de Visser, S. P.; Shaik, S. *J. Am. Chem. Soc.* **2003**, *125*, 8698−8699.

(15) (a) Quinonero, D.; Morokuma, K.; Musaev, D. G.; Mas-Balleste, R.; Que, L., Jr. *J. Am. Chem. Soc.* **2005**, *127*, 6548−6549. (b) Chen, K.; Costas, M.; Kim, J.; Tipton, A. K.; Que, L., Jr. *J. Am. Chem. Soc.* **2002**, *124*, 3026−3035. (c) Chen, K.; Que, L., Jr. *J. Am. Chem. Soc.* **2001**, *123*, 6327−6337. (d) Lehnert, N.; Fujisawa, K.; Solomon, E. I. *Inorg. Chem.* **2003**, *42*, 469−481. (e) Lehnert, N.; Ho, R. Y. N.; Que, L., Jr.; Solomon, E. I. *J. Am. Chem. Soc.* **2001**, *123*, 8271−8290. (f) Lehnert, N.; Ho, R. Y. N.; Que, L., Jr.; Solomon, E. I. *J. Am. Chem. Soc.* **2001**, *123*, 12802−12816. (g) Bassan, A.; Blomberg, M. R. A.; Siegbahn, P. E. M.; Que, L., Jr. *J. Am. Chem. Soc.* **2002**, *124*, 11056−11063. (h) Solomon, E. I.; Brunold, T. C.; Davis, M. I.; Kemsley, J. N.; Lee, S.-K.; Lehnert, N.; Neese, F.; Skulan, A. J.; Yang, Y.-S.; Zhou, J. *Chem. Rev.* **2000**, *100*, 235−350.

(16) Sharma, P. K.; Kevorkiants, R.; de Visser, S. P.; Kumar, D.; Shaik, S. *Angew. Chem., Int. Ed.* **2004**, *116*, 1149−1152.

(17) (a) Ortiz de Montellano, P. R. *Acc. Chem. Res.* **1998**, *31*, 543−549. (b) Ortiz de Montellano, P. R. *Curr. Opin. Chem. Biol.* **2000**, *4*, 221−227. (c) Schuller, D. J.; Wilks, A.; Ortiz de Montellano, P. R.; Poulos, T. L. *Nat. Struct. Biol.* **1999**, *6*, 860−867.

(18) For O−O homolysis followed by C−H hydroxylation in P450, see: (a) White, R. E.; Sligar, S. G.; Coon, M. J. *J. Biol. Chem.* **1980**, *255*, 11108−11111. For competition between O−O homolysis and heterolysis in heme enzymes, see: (b) Allentoff, A. J.; Bolton, J. L.; Wilks, A.; Thompson, J. A.; Ortiz de Montellano, P. R. *J. Am. Chem. Soc.* **1992**, *114*, 9744−9749. (c) Groves, J. T.; Watananbe, Y. *J. Am. Chem. Soc.* **1988**, *110*, 8443−8452. (d) Yamaguchi, K.; Watanabe, Y.; Morishima, I. *J. Am. Chem. Soc.* **1993**, *115*, 4058−4065. (e) Shimizu, T.; Murakami, Y.; Hatano, M. *J. Biol. Chem.* **1994**, *269*, 13296−13304. For competition between O−O homolysis and heterolysis in nonheme species, see: (f) Kaizer, J.; Costas, M.; Que, L., Jr. *Angew. Chem., Int. Ed.* **2003**, *42*, 3671−3673. (g) Robert, A.; Coppel, Y.; Meunier, B. *J. Chem. Soc., Chem. Commun.* **2002**, 414−415. (h) Lenhert, N.; Ho, R. Y. N.; Que, L., Jr.; Solomon, E. I. *J. Am. Chem. Soc.* **2001**, *123*, 8271−8290.

(19) Chandrasena, R. E. P.; Vatsis, K. P.; Coon, M. J.; Hollenberg, P. F.; Newcomb, M. *J. Am. Chem. Soc.* **2004**, *126*, 115−126.

(20) Harris, D. L.; Loew, G. H. *J. Am. Chem. Soc.* **1996**, *118*, 10588−10594.

(21) Ensing, B.; Buda, F.; Baerends, E. J. *J. Phys. Chem. A* **2003**, *107*, 5722−5731.

(22) (a) Fujita, M.; Costas, M.; Que, L., Jr. *J. Am. Chem. Soc.* **2003**, *125*, 9912−9913. (b) Ensing, B.; Baerends, E. J. *J. Phys. Chem. A.* **2002**, *106*, 7902−7910. (c) Ensing, B.; Buda, F.; Blöchl, P.; Baerends, E. J. *Angew. Chem., Int. Ed.* **2001**, *40*, 2893−2895.

Scheme 2. Probe Substrate, **1**, and Its Two Oxidation Products by P450

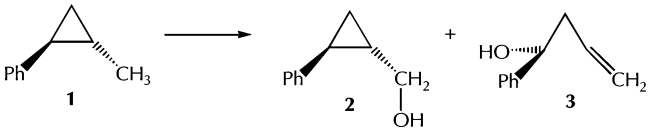

Based on the above considerations it was deemed necessary to use DFT calculations to assess the relative reactivity of the three species of P450, in Scheme 1, with an aim of contributing to the resolution of the identity of the P450 oxidant species. The target reaction was chosen to be C−H hydroxylation of the radical probe substrate in Scheme 2, *trans*-2-phenylmethylcyclopropane, **1**, which gives rise to the alcohol products **2** and **3**; **2** is an unrearranged alcohol that conserves the same structure as the parent substrate, while **3** is a rearranged alcohol which is formed as a minor product (up to 30%) of the oxidation.[23] The ratio [**2**/**3**] is commonly used to clock the lifetime of the radical after hydrogen abstraction from **1**, by a hydrogen abstractor reagent like Cpd I, and therefore the reactivity patterns of **1** provide important mechanistic insight into the oxidation process. There are also kinetic isotope effect (KIE) data for the P450 oxidation of **1**, and these may serve as probes of the oxidant species. As such, the key questions that we intend to answer in the present contribution are the following: (a) Are Cpd 0 and/or Fe(H_2O_2) competitive enough to react with the clock in the presence of Cpd I[24] and affect the mechanistic conclusions that derive from the results? And if not, can Cpd 0 and/or Fe(H_2O_2) be responsible for the sluggish reactivity in the absence of Cpd I or when the latter is formed slowly as might be the case in the T252A mutant? Kinetic isotope effect (KIE) values will be calculated for these mechanisms as potential probes of the reactivity of the three reagents.

Methods

Systems: The hydroxylation of **1** with a Cpd I model was studied by us recently,[24] and it was found to involve two-state reactivity (TSR),[25] nascent from the two low lying spin states of Cpd I; the doublet state was found to lead to the unrearranged product, **2**, while the quartet spin state was found to generate the rearranged alcohol product, **3**. To be consistent,[24] here too, we used model P450 complexes, in which we replaced the cysteinate ligand by HS^- and simplified the native porphyrin to porphine. The effect of hydrogen bonding to the thiolate ligand[26] was estimated, as before,[27] using two ammonia molecules, which donate two NH- - -S bonds to sulfur ($r_{N- - -S}$ = 2.66 Å).

Methods and Basis Sets: All calculations were carried out with the hybrid B3LYP functional,[28] using the double-ζ LACVP basis set[29] for geometry optimization and frequency calculations. As shown previously,[16] the O−O bond energy and cleavage barrier are sensitive to polarization functions, and therefore subsequent single-point calculations were done with the larger basis set, LACV3P^{+}*. Further corrections to the energy included the zero-point energy correction (ZPC), the effect of bulk polarity, which was calculated using a solvent model with a dielectric constant $\epsilon = 5.7$ and a probe radius of 2.72 Å, and the effect of two NH- - -S bonds to sulfur ($r_{N- - -S}$ = 2.66 Å).[27]

Transition states were located after an initial scan of the reaction path along a given coordinate, while other degrees of freedom were fully optimized. Energies were scanned along two reaction coordinates; a scan along the O−H distance led to a concerted O−O homolysis and hydrogen abstraction, while a scan along the O−O distance led to the stepwise mechanisms whereby the bound OH radical is initially formed and subsequently abstracts a hydrogen from the substrate. For each scan, the topmost point was subjected to a transition state search, and the optimized transition structure was subsequently verified by frequency calculations.

KIEs were calculated as before[24] using the semiclassical Eyring equation with subsequent Wigner correction for tunneling. In the mechanisms that involved hydrogen abstraction by the OH radical, the potential energy was very flat. We therefore ran a transition state location using the larger basis set LACVP** and recalculated the KIE values. With an attempt to determine reliable KIE values for the hydrogen abstraction steps with the Cpd 0 and Fe(H_2O_2) reagents, we also studied the hydrogen abstraction reaction of **1** with a free OH radical using UB3LYP/6-31G and UB3LYP/6-31G**. However, in all the cases, the barriers were very small and the KIE values using harmonic frequencies were not reliable.

All geometry optimizations, single-point energy calculations, and solvent and hydrogen bonding corrections were done with the JAGUAR 5.5 package.[30] The frequency calculations and ZPE corrections were performed with GAUSSIAN 98 and 03 packages.[31]

Results

The study generated a significant amount of data that are summarized in the Supporting Information (SI). The key relevant data are displayed in this section. Before going over the results, we note that, for Cpd 0, the ground state is a doublet spin state, and the quartet state lies significantly higher (10 kcal/mol or more).[13a] As such, for Cpd 0 we calculated the profiles for the doublet state only. By contrast, the Fe(H_2O_2) complex has a low lying quartet state, and hence we calculated the energy profiles of substrate oxidation for both the doublet and quartet states. As it turned out (see later Figure 5), the quartet state surface is too high to matter also for Fe(H_2O_2).

A. OO Bond Homolysis Behavior of Cpd 0 and Fe(H_2O_2). The homolytic behavior of Cpd 0 of P450, communicated before,[16] is presented here in Figure 1a, while Figure 1b shows the analogous behavior of the Fe(H_2O_2) complex. Inspection of Figure 1a shows that the concerted mechanism possesses a very high barrier.[16,32] A lower energy mechanism involves initial O−O homolysis to form *a bound OH radical*[16] that instantly attacks the *meso* position of the porphine in a HO-like manner. Figure 1b shows the preferred homolysis mechanism nascent from the Fe(H_2O_2) complex, and the similarity to the mechanism of Cpd 0 is obvious. The question that follows is how would the mechanism change in the presence of the substrate **1**, and will it involve now substrate hydroxylation?

(23) Newcomb, M.; Toy P. H. *Acc. Chem. Res.* **2000**, *33*, 449−455.
(24) Kumar, D.; de Visser, S. P.; Sharma, P. K.; Cohen, S.; Shaik, S. *J. Am. Chem. Soc.* **2004**, *126*, 1907−1920.
(25) (a) Shaik, S.; Filatov, M.; Schröder, D.; Schwarz, H. *Chem.*−*Eur. J.* **1998**, *4*, 193−199. (b) Shaik, S.; de Visser, S. P.; Schwarz, H.; Schröder, D. *Curr. Opin. Chem. Biol.* **2002**, *6*, 556−567. (c) Ogliaro, F.; Harris, N.; Cohen. S.; Filatov, M.; de Visser, S. P.; Shaik, S. *J. Am. Chem. Soc.* **2000**, *122*, 8997−8989. (d) Shaik, S.; Cohen. S.; de Visser, S. P.; Sharma, P. K.; Kumar, D.; Kozuch, S.; Ogliaro, F.; Danovich, D. *Eur. J. Inorg. Chem.* **2004**, 207−226.
(26) Poulos. T. L. *J. Biol. Inorg. Chem.* **1996**, *1*, 356−359.
(27) Ogliaro, F.; Cohen, S.; de Visser, S. P.; Shaik, S. *J. Am. Chem. Soc.* **2000**, *122*, 12892−12893.
(28) (a) Becke, A. D. *J. Chem. Phys.* **1992**, *96*, 2155−2160. (b) Becke, A. D. *J. Chem. Phys.* **1992**, *97*, 9173−9177. (c) Becke, A. D. *J. Chem. Phys.* **1993**, *98*, 5648−5652. (d) Lee, C.; Yang, W.; Parr, R. G. *Phys. Rev. B* **1988**, *37*, 785−789.
(29) (a) Hay, J. P.; Wadt, W. R. *J. Chem. Phys.* **1985**, *82*, 299−308. (b) Friesner, R. A.; Murphy, R. B.; Beachy, M. D.; Ringlanda, M. N.; Pollard, W. T.; Dunietz, B. D.; Cao, Y. X. *J. Phys. Chem. A* **1999**, *103*, 1913−1928.
(30) *Jaguar 5.5*; Schrödinger, Inc.: Portland, OR, 2003.
(31) (a) Frisch, M. J. et al. *Gaussian 98*, revision A.07; Gaussian, Inc.: Pittsburgh, PA, 1998. (b) Frisch, M. J. et al. *Gaussian 03*, revision B.05; Gaussian, Inc.: Pittsburgh, PA, 2003.
(32) Kamachi, T.; Shestakov, A. F.; Yoshizawa, K. *J. Am. Chem. Soc.* **2004**, *126*, 3672−3673.

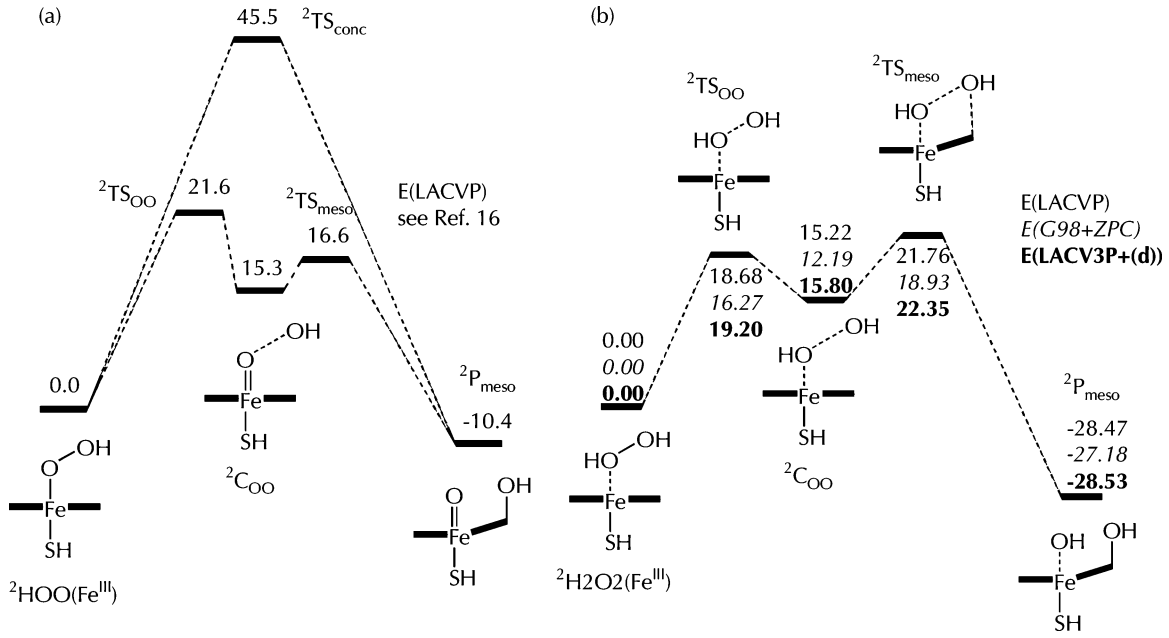

Figure 1. Energy (in kcal/mol) profiles for *meso* hydroxylation of the porphine for (a) concerted and stepwise mechanisms by Cpd 0 (see ref 16) and (b) the stepwise mechanism by Fe(H_2O_2). The porphine is represented by boldface bars flanking the iron.

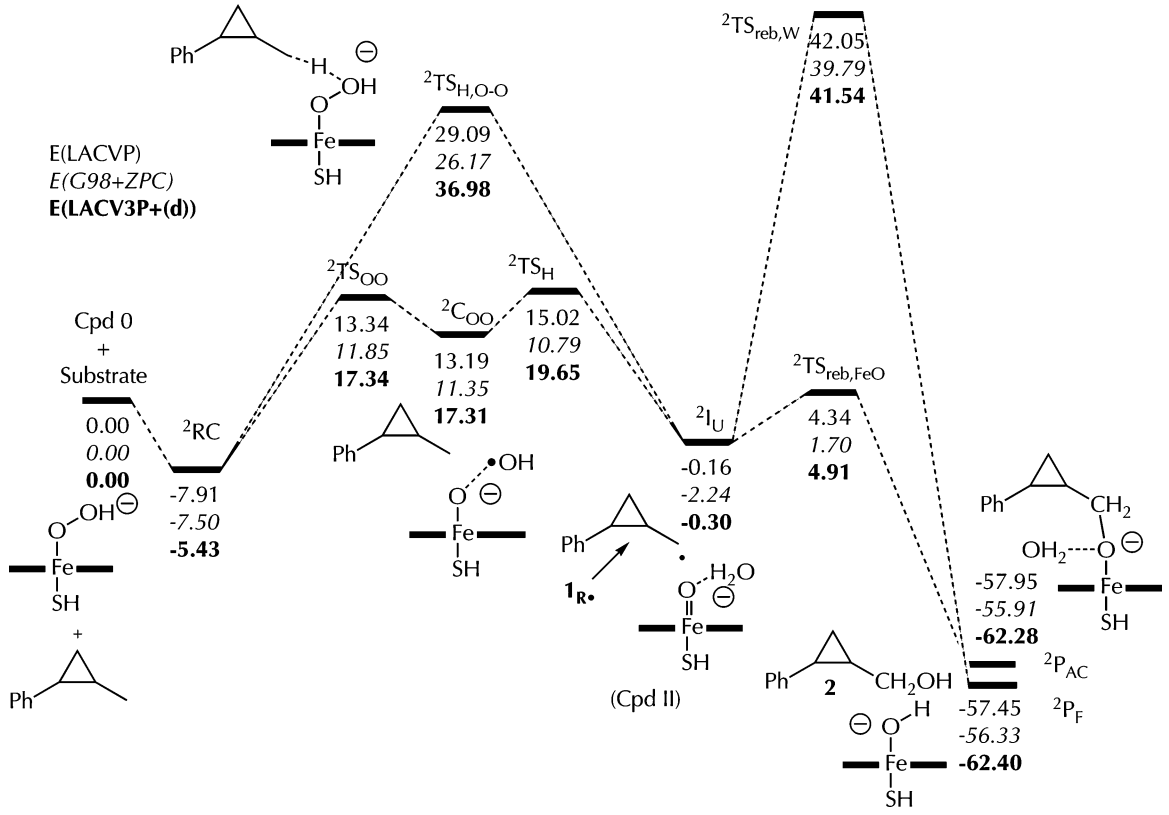

Figure 2. Energy profiles (kcal/mol) showing the hydroxylation of **1** by Cpd 0, via a direct H-abstraction mechanism (upper profile) and a stepwise one following O−O bond homolysis (lower profile). ZPC means zero-point energy correction. The subscript U means "unrearranged".

B. Hydroxylation of 1 by Cpd 0. Figure 2 shows two hydroxylation mechanisms of **1** by Cpd 0: the upper profile is a direct O−O cleavage and hydrogen-abstraction mechanism, and the lower one is a stepwise mechanism. The structures of the corresponding critical species are displayed in Figures 3 and 4.

The direct mechanism, in Figure 2, involves simultaneous O−O cleavage and hydrogen abstraction (H-abstraction) from the substrate **1**; all the structures of the corresponding species are shown in Figure 3. The bond activation transition state, ^{2}**TS**$_{H,O-O}$, leads to the intermediate, ^{2}**I**$_U$, composed of the radical of **1**, **1**$_{R\bullet}$, a water molecule, and the oxo-iron anion complex (Cpd II). Subsequently, the **1**$_{R\bullet}$ species rebounds on the water molecule via ^{2}**TS**$_{reb,w}$; simultaneously the water was found to transfer a hydrogen atom to Cpd II to give the ferric-hydroxo complex and the free alcohol product **2** (^{2}**P**$_F$). The barriers of

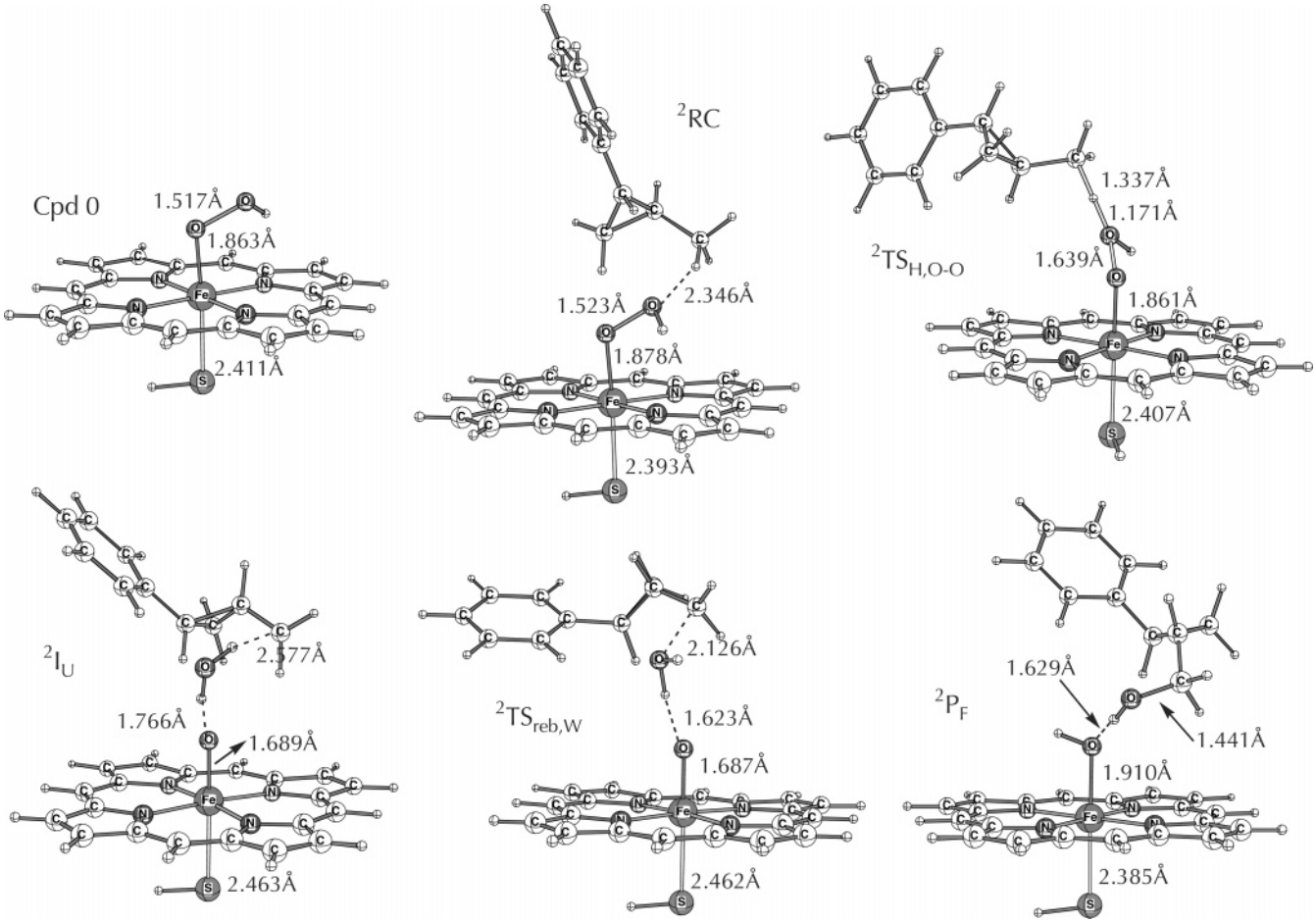

Figure 3. Critical structures for C−H hydroxylation of **1** by Cpd 0 in the direct O−O cleavage/H-abstraction mechanism, described by the upper energy profile in Figure 2.

these two steps are very large. An alternative and lower energy rebound step involves rebound of $\mathbf{1}_{R}$**.** on Cpd II and formation of the alkoxy-ferric complex of **2** ($^2\mathbf{P}_{AC}$). In any event, the direct H-abstraction by Cpd 0 would have a very large barrier, at least ca. 37 kcal/mol (a LACV3P+(d) datum, relative to ^{2}**RC** in Figure 2).

The lower energy mechanism in Figure 2 is stepwise with an initial homolytic O−O bond cleavage via $^2\mathbf{TS}_{OO}$ leading to the $^2\mathbf{C}_{OO}$ intermediate that possesses a bound OH radical coordinated to Cpd II. The OH radical then abstracts a hydrogen atom from **1**, via $^2\mathbf{TS}_{H}$, to form the intermediate ^{2}**I**, which then follows the same rebound mechanism via $^2\mathbf{TS}_{reb,FeO}$ to form the alkoxy complex, $^2\mathbf{P}_{AC}$; the corresponding structures are shown in Figure 4. It is apparent that substrate oxidation via the stepwise O−O homolysis mechanism/H-abstraction is energetically much lower than the one involving direct H-abstraction by Cpd 0. The highest barrier (measured from ^{2}**RC**) to reach $^2\mathbf{TS}_{H}$ is 25.1 kcal/mol at the B3LYP/LACV3P+(d) level; the barrier for the H-abstraction itself is only 2.3 kcal/mol at the same level or 1.8 kcal/mol at the B3LYP/LACVP level. Note that the barrier to O−O homoylsis increases substantially for the LACV3P+(d) basis set; this result is reported below also for the reaction of the Fe(H_2O_2) complex. As noted before,[16] this basis set dependence of the barrier reflects the strengthening of the O−O bond upon inclusion of polarization functions on the oxygen atoms.

C. Hydroxylation of 1 by Fe(H_2O_2). Since the Fe(H_2O_2) complex was found to involve two closely lying spin states, doublet and quartet, we studied the hydroxylation mechanisms from these two states; Figure 5 traces the energy profiles for the direct mechanisms, while the corresponding structures are displayed in Figure 6. Figure 7 depicts the energy profile for the stepwise O−O homolysis/H-abstraction mechanism, while Figure 8 displays the corresponding structures of the critical species.

Figure 5 shows the results for the direct H-abstraction mechanism, whereby the O−O bond cleavage occurs in concert with C−H bond activation, leading to the intermediates $^{4,2}\mathbf{I}_{U}$, which then give rise to the ferric-alcohol complexes of **2**, $^{2,4}\mathbf{P}_{U}$, by rebound of the radical of **1** on the iron-hydroxo complex, via $^2\mathbf{TS}_{reb}$. The intermediates $^{4,2}\mathbf{I}_{U}$ can also rearrange via $^2\mathbf{TS}_{rear}$, to yield the rearranged radical complex intermediates, $^{4,2}\mathbf{I}_{R}$, which subsequently collapse in a barrier-free fashion to the ferric complexes of the rearranged alcohol, ^{2,4}**P**. The rebound barriers are seen to be larger than the rearrangement barriers. Furthermore, Figure 5 shows that the bond activation from the quartet state is much higher than that of the doublet state, and hence the higher spin state was not considered anymore. The corresponding geometries of all the structures are displayed in Figure 6.

Figure 7 describes the stepwise, O−O homolysis/H-abstraction mechanism for the hydroxylation of **1** by Fe(H_2O_2). As in

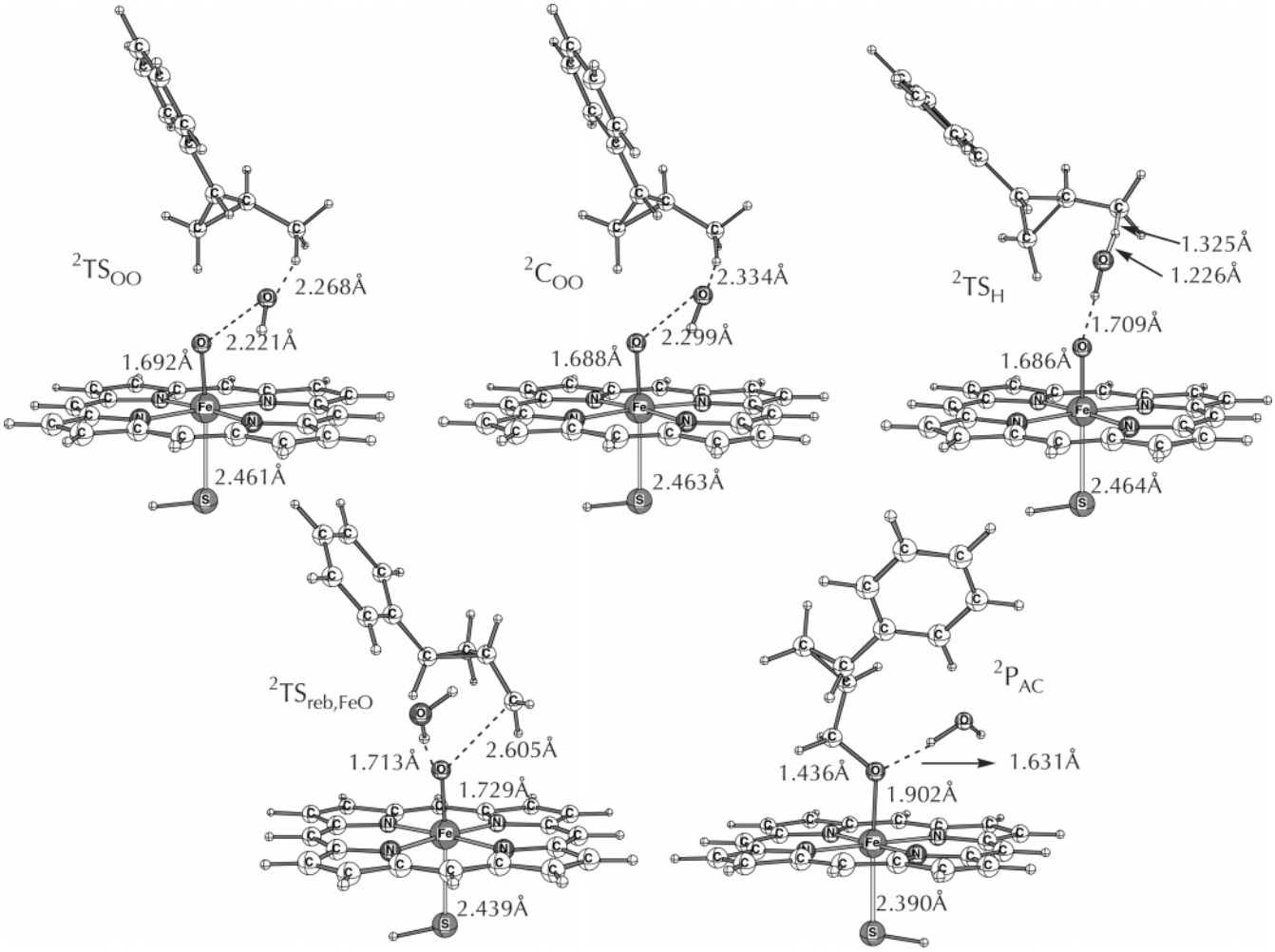

Figure 4. Critical structures for C−H hydroxylation of **1** by Cpd 0 in the stepwise O−O bond homolysis/H-abstraction mechanism, described by the upper energy profile in Figure 2.

Figure 2, here too an initial $^2\mathbf{TS}_{OO}$ species leads to an intermediate, $^2\mathbf{C}_{OO}$, which involves a bound OH radical, an iron-hydroxo complex, and **1**. Subsequently, the bound OH radical abstracts a hydrogen atom from **1**, via $^2\mathbf{TS}_H$, leading to the intermediate $^2\mathbf{I}_U$, which then rebounds to give the alcohol **2**, either free, $^2\mathbf{P}_F$, by rebounding on the water molecule, or complexed to the ferric porphine, $^2\mathbf{P}_{AC}$, by rebounding on the iron-hydroxo complex. Figure 8 depicts geometric features for the key structures.

Comparison of Figure 7 to 5 reveals that, as in the case of Cpd 0, here too the preferred C−H hydroxylation pathway will be the stepwise O−O homolysis/H-abstraction. The highest barrier (relative to $^2\mathbf{RC}$) in this case is 21.0 kcal/mol (LACV3P+(d) datum in Figure 7) and corresponds to the bond homolysis step via $^2\mathbf{TS}_{OO}$. The subsequent H-abstraction barrier via $^2\mathbf{TS}_H$ is negligible of the order of less than 0.1 kcal/mol.

D. Acid-Catalyzed Hydroxylation of 1 by Cpd 0. In an attempt to probe the effect of acid catalysis on the reactivity of Cpd 0, we used the cluster $NH_4^+(H_2O)_2$ coordinated to Cpd 0. As may be seen from Figure 9, optimization of the cluster led to the spontaneous protonation of Cpd 0 to Fe(H_2O_2); apparently the distal position of Cpd 0 is basic enough to abstract a proton very fast.[16,20] Thus, the oxidant here is Fe(H_2O_2) hydrogen-bonded to a cluster of ammonia and two waters. As before, here too, the stepwise O−O homolysis/H-abstraction mechanism is the preferred mechanism. The barrier (from $^2\mathbf{RC}$) for O−O homolysis is 21.7 kcal/mol, and the subsequent barrier is 1.4 kcal/mol; values which are very similar to the ones in Figure 7 for hydroxylation by bare Fe(H_2O_2). The rebound barrier from $^2\mathbf{I}_U$ toward the ferric-alcohol product, $^2\mathbf{P}_{AC}$, vanishes however compared with Figure 7. Since there is not much that is new about the structures for this mechanism, and since the cluster $NH_3(H_2O)_2$ may not be a realistic environment for P450, we do not show the structures here and refer the interested readers to the SI (Figures S.1−S.9).

E. Uncoupling Reactions of Cpd 0 and Fe(H_2O_2) and Other Competing Processes. The abilities of either Cpd 0 and/or Fe(H_2O_2) to oxidize the substrate depend, among other things, on whether the barriers for C−H hydroxylation are smaller or higher than the dissociation of these reagents to give OOH^- and H_2O_2, namely the uncoupling reactions, eqs 1 and 2.[2]

$$\text{Cpd 0 (Por(HS)FeOOH}^-) \rightarrow \text{HOO}^- + \text{Por(HS)Fe} \quad (1)$$

$$\text{Por(HS)Fe(HOOH)} \rightarrow \text{HOOH} + \text{Por(HS)Fe} \quad (2)$$

To gauge this competition we calculated the bond dissociation energies (BDEs) for Cpd 0 and Fe(H_2O_2), and the results are collected in Table 1. These BDEs should be compared to the O−O homolysis barriers (relative to the free reactants), which are also tabulated in Table 1 (values from Figures 7 and 2). It

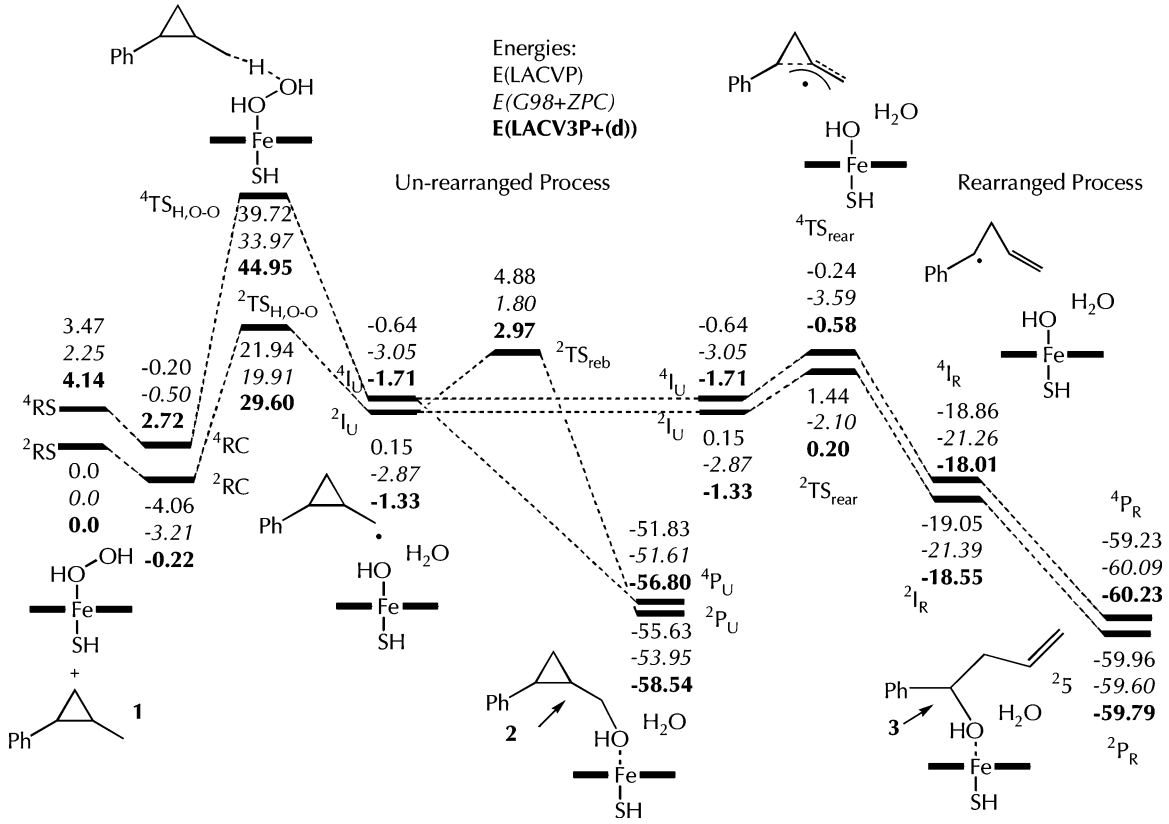

Figure 5. C−H hydroxylation of **1** by Fe(H_2O_2) via the direct O−O cleavage/H-abstraction mechanisms in the doublet and quartet states. Also shown are the corresponding rearrangement mechanisms. The subscripts U and R correspond to "Unrearranged" and "Rearranged", respectively.

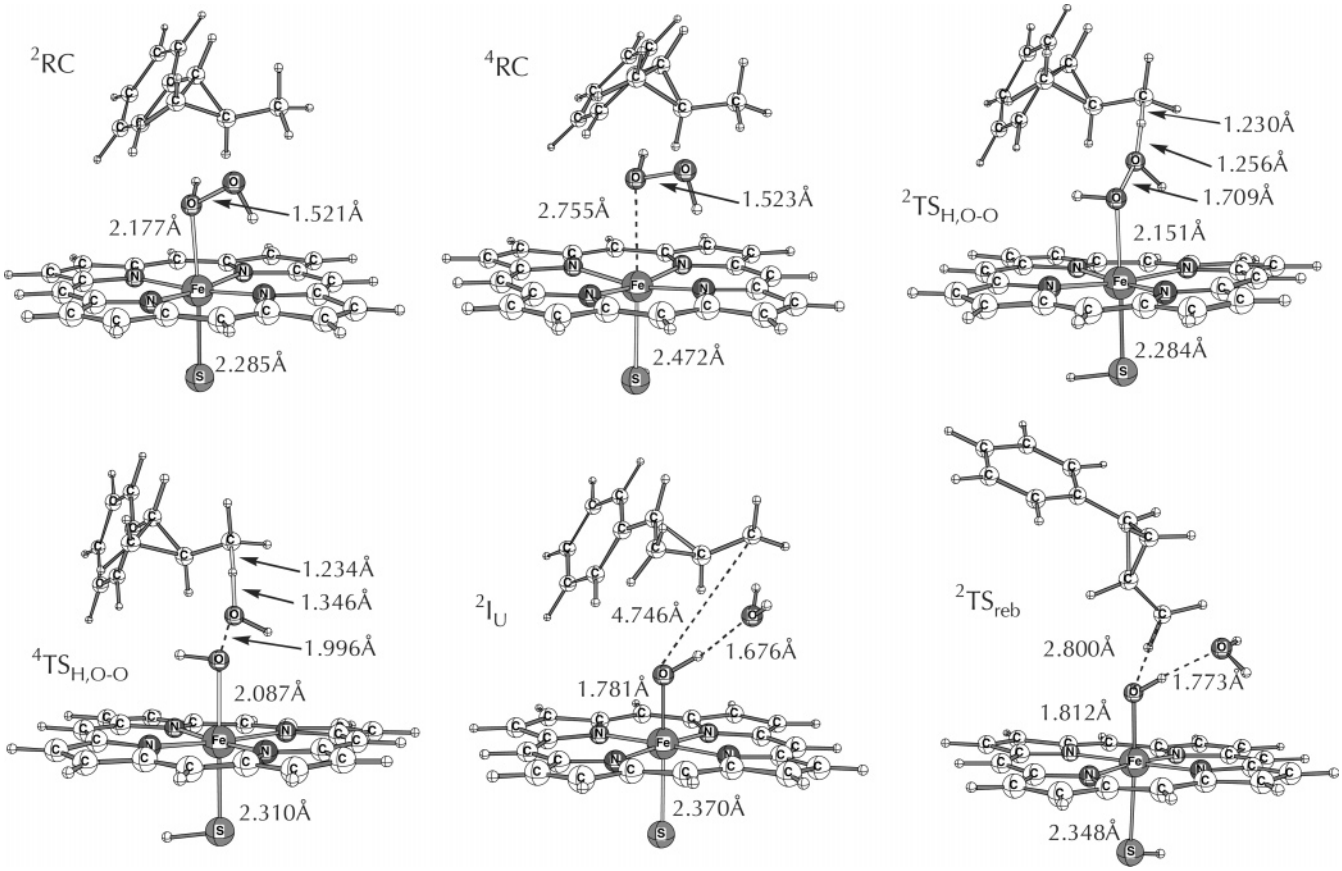

Figure 6. Key geometric features of a few structures during the direct O−O cleavage/C−H hydroxylation of **1** by Fe(H_2O_2) in the doublet and quartet states described in Figure 5.

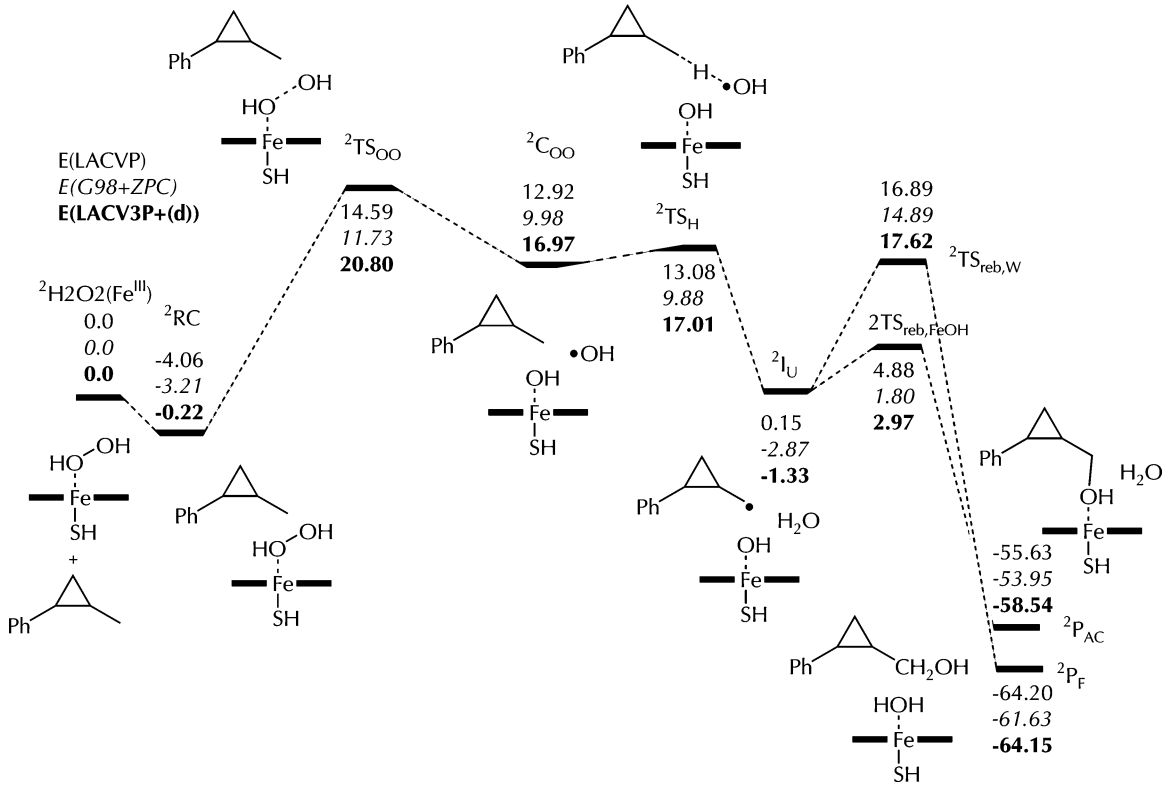

Figure 7. C−H hydroxylation of **1** by Fe(H_2O_2) via the stepwise O−O homolysis/H-abstraction mechanism.

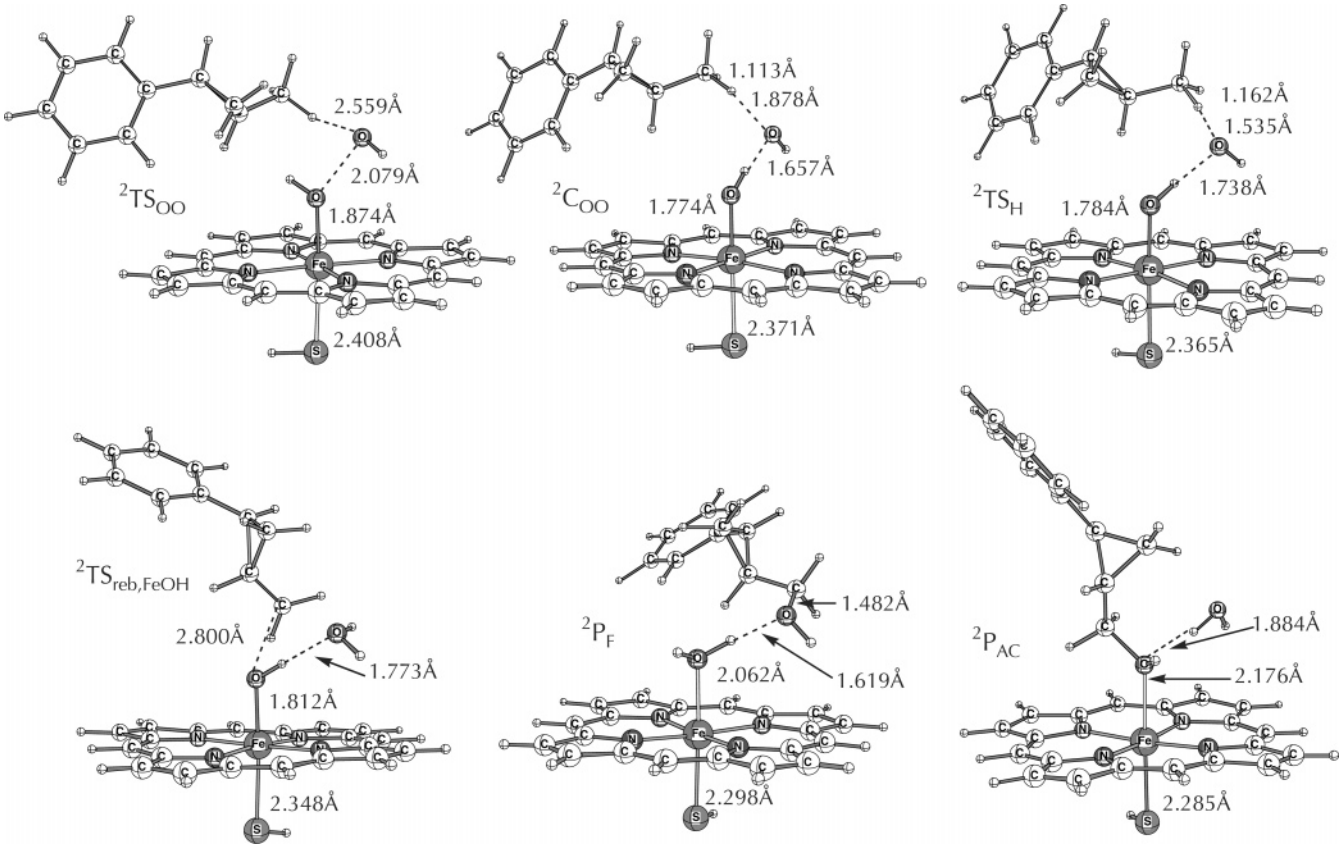

Figure 8. Key geometric features of structures during C−H hydroxylation of **1** by Fe(H_2O_2) via the stepwise O−O homolysis/H-abstraction mechanism described in Figure 7.

is seen that for both oxidants the higher spin states, the quartet and sextet states, have smaller BDEs than the low spin states. In the case of Fe(H_2O_2) the barrier for oxidation from the quartet state of Fe(H_2O_2) in Figure 5 is much higher than the corresponding BDE, and therefore this state will not participate in oxidation. However the BDE(Fe−H_2O_2) for the doublet state

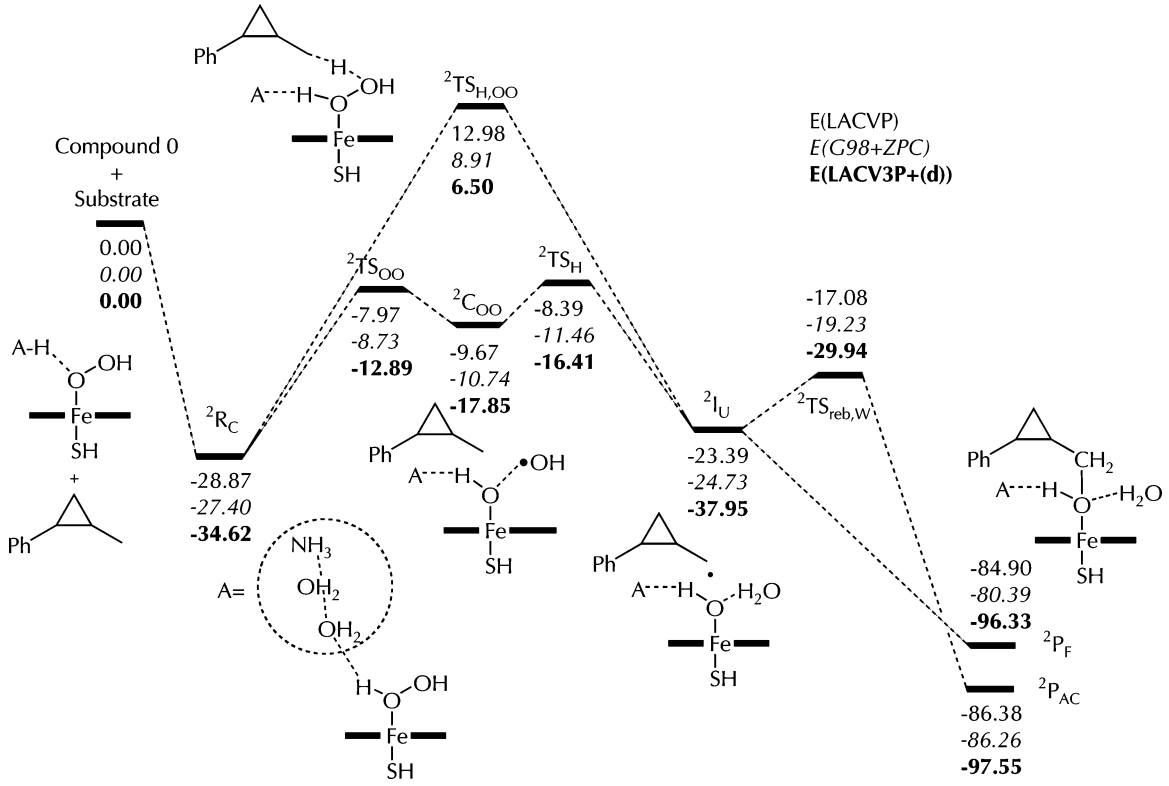

Figure 9. Direct and stepwise mechanisms for C−H hydroxylation of **1** by Cpd 0 and an acid cluster $NH_4^+(H_2O)_2$. The letter A symbolizes ammonia and two water molecules.

Table 1. Bond Dissociation Energy (BDE) Values and O−O Homolysis Barriers for Cpd 0 and $Fe(H_2O_2)$[a]

	BDE (BDE + ZPE)[b] $Fe(H_2O_2)$	BDE (BDE + ZPE)[b] Cpd 0	$\Delta E^{\neq}_{O-O}$[b,d] $Fe(H_2O_2)$	$\Delta E^{\neq}_{O-O}$[b,d] Cpd 0
doublet	12.1 (10.3)	74.8 (73.0); 38.8[c]	14.6 (11.7)	13.3 (11.9)
	10.1	57.3	20.8	17.3
quartet	7.4 (6.0)	59.0 (57.6); 22.3[c]	not calcd	not calcd
	4.6	42.2		
sextet	7.4 (6.0)	62.4 (60.9); 25.7[c]	not calcd	not calcd
	4.3	43.6		

[a] Values in kcal/mol; all values here and elsewhere are rounded to the first decimal. [b] The upper value corresponds to LACVP, and the lower one, to LACV3P+(d). [c] This is an LACVP datum with correction due to bulk polarity using a dielectric constant, $\epsilon = 5.7$. [d] The O−O homolysis barriers are taken from Figures 2 and 7. These values are measured from the reactants to offset the interactions of the oxidant with the substrate. This is particularly strong for Cpd 0 in Figure 2.

is higher than the values for the higher spin states. Furthermore, the value of BDE(Fe−H_2O_2) is still smaller by ca. 2 than the O−O homolysis barrier in Figure 7 (LACVP with ZPE), suggesting that only a small fraction of the $^2Fe(H_2O_2)$ will be able to participate in oxidation; the rest will lead to uncoupling and release of H_2O_2. Using simply Boltzmann factors, this fraction would be less than 1%, but since uncoupling (eq 2) is reversible while the competing O−O homolysis (in Figure 7) is not, the percentage of substrate oxidation may be higher.

For Cpd 0, however, the BDE(^{2}Fe−OOH$^-$) datum is large, and while this value is reduced by half, when bulk polarity correction is included, still the BDE(^{2}Fe−OOH$^-$) is larger than the O−O homolysis barrier. Consequently, the ^{2}Cpd 0 species will participate in principle in substrate oxidation preferentially more than in uncoupling.

Table 2 displays the barriers leading to C−H hydroxylation of **1** in the O−O homolysis/H-abstraction mechanisms of Cpd

Table 2. Energy Barriers (in kcal/mol) for C−H Hydroxylation of **1** by Cpd I, Cpd 0, and $Fe(H_2O_2)$

barrier	Cpd I[a]	Cpd 0[b]	$Fe(H_2O_2)$[c]
LACVP	19.4	22.9	18.7
LACVP+ZPC	15.2	18.3	14.9
LACV3P+(d)	17.0	25.1	21.0
LACVP+ZPC+2NH...S+ϵ=5.7	18.3	23.8	17.3
LACV3P+(d)+ZPC+2NH...S+ϵ=5.7	16.0	25.9	19.6

[a] From ref 24, but the barriers are calculated from ^{2}RC (instead of the separate reagents in the original paper). [b] Relative to ^{2}**RC**, From Figure 2. [c] Relative to ^{2}**RC**, From Figure 7.

0 and $Fe(H_2O_2)$, in Figures 2 and 7. These data are compared with the barrier for the hydroxylation of **1** by the low-spin state of Cpd I.[24] The latter values differ slightly from the ones obtained before[24] since here we take all barriers from the reaction complexes, ^{2}**RC**, which involve a weak interaction of Cpd I with the substrate. The comparison of the barriers is done at different levels, up to the highest one, LACV3P+*, with all corrections: ZPC, polarity effects, and hydrogen bonding to the thiolate ligand. As already argued, the LAVCP basis set underestimates the O−O bond energies and homolysis barriers[16] in the reactions of Cpd 0 and $Fe(H_2O_2)$, while the LACV3P+* basis set, which includes polarization functions, rectifies this deficiency. Therefore, the discussion of the data in Table 2 is limited to the highest level. It is apparent that at the highest level the most reactive species is Cpd I, with a lower barrier than those for Cpd 0 and $Fe(H_2O_2)$, by 9.9 and 3.6 kcal/mol, respectively. Thus, when Cpd I is present the reactivity of the Cpd 0 would be negligible. The barrier for $Fe(H_2O_2)$, compared with that for Cpd I, indicates that the former species will exhibit a small amount of substrate oxidation in the presence of Cpd I, but the total yield of this process is expected to be smaller than what is suggested by the relative barriers, since the $Fe(H_2O_2)$

Table 3. Barriers (in kcal/mol) for Competing Processes during Oxidation of **1** by Cpd 0 and Fe(H_2O_2)

reaction type	LACVP	LACV3P+(d)
a − Cpd 0		
1a − *meso* attack (Figure 1a)	1.3	not calcd
2a − H-abstraction (Figure 2)	1.8	2.3
3a − rebound (Figure 2)	4.5 (0)	5.2 (0)
4a − rearrangement [a]	1.3	1.5
b − Fe(H_2O_2)		
1b − *meso* attack (Figure 1b)	6.5	6.5
2b − H-abstraction (Figure 7)	0.2 (1.3)[b]	0.04 (1.4)[b]
3b − rebound (Figure 7)	4.8	4.4
4b − rearrangement (Figure 5)	1.3	1.5

[a] The barrier for the free radical rearrangement is 0.8 kcal/mol,[24] close to the barriers in entry 4b. Therefore, identical barriers are used for entries 4a and 4b. [b] In parentheses are given the values corresponding to the acidic network assisted mechanism (see Figure 9).

reagent will lead predominantly to uncoupling and generation of free H_2O_2. In the absence of Cpd I, however, we should consider Cpd 0 and Fe(H_2O_2) as viable albeit sluggish oxidants compared with Cpd I.

Table 3 collects the barriers for *meso* hydroxylation of the porphine (Figure 1), which competes with substrate oxidation, after the O−O bond has been homolyzed and the bound OH radical was generated. In addition, we show here barriers for rebound and rearrangement of the radical generated from **1** (**1**$_{R\bullet}$).

For Cpd 0 (FeOOH), the barrier for H-abstraction is slightly larger than the corresponding barrier for *meso* hydroxylation (entry 1a vs 2a). This means that even if Cpd 0 undergoes O−O bond homolysis in preference to uncoupling (HOO^- dissociation), the intermediate ^{2}**C**$_{OO}$ in Figure 2 would undergo a slightly faster attack on the *meso* position of the porphyrin rather than a H-abstraction from the substrate. Based on the LACVP datum, a rough estimate is that 15% of the bound OH radical will oxidize the substrate and the rest will carry porphyrin oxidation.

In the case of Fe(H_2O_2), the H-abstraction barriers are significantly smaller than the barriers for *meso* hydroxylation (entries 1b and 2b). Therefore, most (>90%) of the bound OH radical in ^{2}**C**$_{OO}$ (Figure 7) will perform substrate oxidation. We recall, however, that the Fe(H_2O_2) species participates only to a small extent in substrate oxidation due to more efficient uncoupling (loss of H_2O_2).

Table 3 shows also barriers for the rebound of the radical, **1**$_{R\bullet}$, to form an alcohol and for rearrangement of the radical (see Figure 6). It is seen that with both reagents in Table 3 the rearrangement barriers are smaller than the rebound barriers. Therefore, in both cases most of the oxidized substrate will be the rearranged alcohol **3** (Scheme 2).

Since the barriers for H-abstraction by the bound OH radical are very small, 0.2−1.8 kcal/mol, we decided to investigate the KIE behavior of a free OH radical with the substrate **1**. Table 4 collects the KIE values for the free OH and the other oxidants. Inspection of the data in entry 1 shows that the KIE is highly dependent on the basis set and can range between 5.0 and 1.8; the large value corresponds to a barrier of 1.3 kcal/mol, and the small value, to 0.1 kcal/mol. With these small barriers the surface is extremely flat, and changes in the basis set or method can induce a shift in the transition state and a corresponding change in the KIE. In addition, such a flat surface is extremely anharmonic, and the use of harmonic frequencies introduces an error[33] in the semiclassical (and Wigner corrected) KIE value.

Table 4. KIE (**1**-CH_3/**1**-CH_2D) Values for H-Abstraction by Different Oxidants

oxidant[a]	semiclassical, LACVP (LACVP**)	Wigner corrected LACVP (LACVP**)
1. free HO•[b]	4.97 (1.81)	6.00 (1.82)
2. Cpd 0[c]	7.0 (6.9)	10.3 (9.5)
3. Fe(H_2O_2)[d]	1.78 (1.73)	1.79 (1.73)
4. Cpd I[e]	6.7	8.35

[a] For entries 2 and 3, the KIE is determined relative to ^{2}**C**$_{OO}$. [b] The barrier is 1.3 (0.1) kcal/mol [c] The barrier for H-abstraction is 1.8 (1.4) kcal/mol [d] The barrier for H-abstraction is 0.2 (0.1) kcal/mol. [e] The LACVP barrier is 19.4 kcal/mol. From ref 24, refers to **1**-CH_3/**1**-CH_2D at T = 298 K.

Indeed, one can see that the KIE values for Cpd 0 and Fe(H_2O_2) vary between 1.8 and 7.0, while in both cases the barrier for H-abstraction is very small, less than 2 kcal/mol. Thus, these values are not reliable, and instead we should gauge the KIE against known experimental and high level ab initio theoretical values. H-abstraction from methane by OH radical is a well-known reaction with a barrier of ca. 7−8 kcal/mol,[34a] an experimental KIE value of 7.1,[35] and a theoretical value of 8.26.[34b] Butane is a more reactive substrate compared with methane and having a weaker C−H bond and a smaller barrier for H-abstraction; the corresponding KIE value was determined[36] using gas phase flash photolysis as 3.8. For a substrate like cyclohexane, with virtually the same C−H bond strength as that in butane, a KIE datum ([C_6H_{12}/C_6D_{12}]) of ∼2 was estimated for the O−O homolysis/C−H abstraction mechanism in the peroxide dependent P450 hydroxylation of cyclohexane.[18a] Based on these values, and since the C−H bond strength in **1** is smaller than that in cyclohexane, the diagnostic KIE for the reactions of the bound OH radical, generated from homolysis of Cpd 0 or Fe(H_2O_2), with the rather reactive substrate **1** is in the range of 2 or even slightly less. The experimental KIE values[37] for C−H hydroxylation by Cpd I are much larger, and the computed data for **1** in Table 4[24] are 6.7 (8.35); these large values mirror the larger H-abstraction barrier of Cpd I compared with the barriers for reactions with OH radical.

Discussion

The data in Tables 1 and 2 define a clear reactivity scenario of the three reagents, Cpd I, Cpd 0, and Fe(H_2O_2). As such, two factors shape the competition; one is the relative barriers for C−H activation, and the other is the competition between O−O homolysis and uncoupling for Cpd 0 and Fe(H_2O_2).

Looking at the relative barriers for C−H activation of **1**, it is clear that Cpd I is the most reactive species, much more so than Cpd 0. The latter will not exhibit any reactivity in the presence of Cpd I. The C−H activation barrier for the Fe(H_2O_2) reagent is 3.6 kcal/mol higher than that for Cpd I, at the highest computational level. This means that, for equimolar concentrations of the two reagents, the amount of oxidation by Fe(H_2O_2)/Cpd I would be 1/99%. The ratio will be even less in favor of Fe(H_2O_2) if we recall that this reagent undergoes more than 90% uncoupling reaction and releases H_2O_2. We may therefore

(33) Hu, W.-P.; Truhlar, D. G. *J. Am. Chem. Soc.* **1995**, *117*, 10726−10734.
(34) (a) Melissas, V. S.; Truhlar, D. G. *J. Chem. Phys.* **1993**, *99*, 1013−1027. (b) Melissas, V. S.; Truhlar, D. G. *J. Chem. Phys.* **1993**, *99*, 3542−3552.
(35) Glereczak, T.; Talkudar, B. K.; Herndon, S. C.; Vaghjiani, G. L.; Ravishankar, A. R. *J. Phys. Chem. A* **1997**, *101*, 3125−3134.
(36) Paraskevopoulos, G.; Nip, W. S. *Can. J. Chem.* **1980**, *58*, 2146−2149.
(37) (a) Groves, J. T.; McClusky, G. A.; White, R. E.; Coon, M. J. *Biochem. Biophys. Res. Commun.* **1978**, *81*, 154−160. (b) Sorokin, A.; Robert, A.; Meunier, B. *J. Am. Chem. Soc.* **1993**, *115*, 7293−7299.

Scheme 3. Oxidative Reactivity Scenario of Cpd 0 and Fe(H_2O_2) in C−H Hydroxylation of **1**

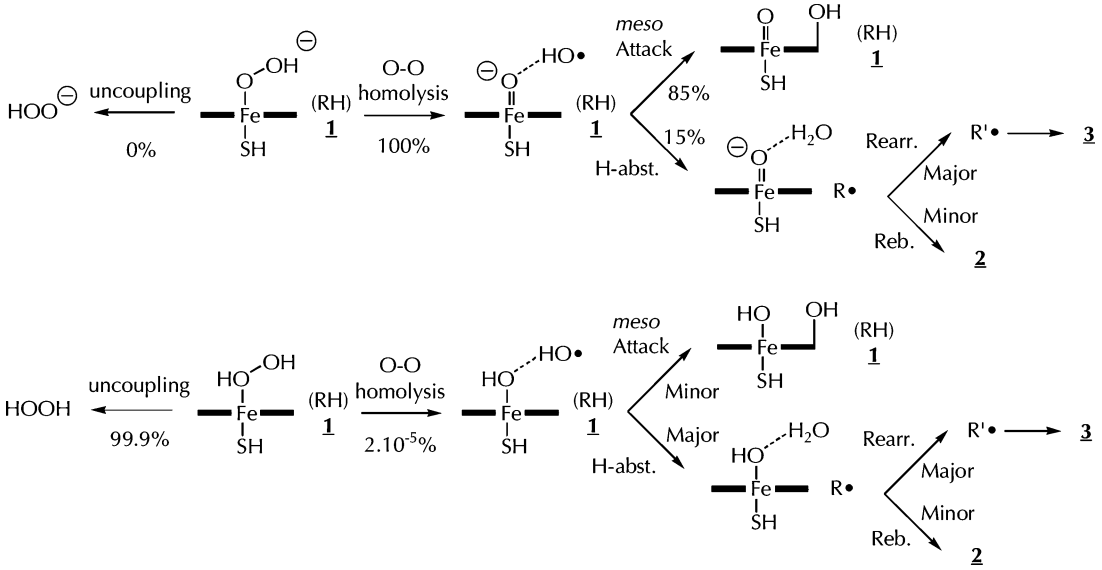

conclude that, in the wild-type enzyme, *C−H hydroxylation will be dominated by Cpd I and will proceed via the classical* "*rebound mechanism*",[9] *with two reactive states (TSR)*[24,25] *leading to products*; the other two reagents will be completely silent.

In the absence of Cpd I, or when its formation is slowed as in the proton-relay mutants of P450,[2] we can anticipate some oxidative reactivity of Cpd 0 and Fe(H_2O_2) in competition with uncoupling. This reactivity will be sluggish due to the higher barriers compared with Cpd I. Scheme 3 summarizes these mechanisms based on the data in Tables 1−3. The mechanisms revealed by the computations are analogous to experimentally deduced ones.[18a,c]

The fractionation of the mechanisms in Scheme 3 is based on simple Boltzmann factors. As a rule: (a) the relative *BDE* vs O−O homolysis barrier will determine the fraction of uncoupling, (b) the relative H-abstraction barrier to *meso* hydroxylation barrier determines the partition of the OH radical between substrate oxidation and autoxidation, and (c) the relative barriers for rebound vs rearrangement determine the ratio **2**/**3** of the unrearranged to rearranged alcohol products.

It is seen that Cpd 0 would proceed to oxidize the substrate and will participate much less in uncoupling and generation of HOO^-. Substrate oxidation will occur via a stepwise mechanism involving O−O homolysis followed by H-abstraction. The bound OH radical due to O−O homolysis will be partitioned between porphyrin oxidation and H-abstraction from **1**, in a 85/15% ratio; in the case of *meso* substituted porphyrins we may anticipate nitrogen hydroxylation as observed by Groves and Watanabe[18c] in peracid dependent oxidations of a model ferric−porphyrin complex. The 15% production of the radical of **1** (R•, in Scheme 3) will produce mostly the rearranged product, **3**.

Unlike Cpd 0, Fe(H_2O_2) will participate mostly in uncoupling and will produce free H_2O_2. A small fraction of the reagent will be dedicated to the oxidation of **1**, showing negligible porphyrin oxidation. The general outline of the substrate oxidation mechanism is very similar to the experimentally deduced one in peroxyphenylacetic acid dependent oxidation by $P450_{LM2,LM4}$. As in the case of oxidation by Cpd 0, above, with Fe(H_2O_2), the substrate oxidation will form mostly the rearranged alcohol product, **3**.

The percentage of substrate oxidation due to the Fe(H_2O_2) complex is calculated in Scheme 3 using Boltzmann factors. As we already noted this underestimates the actual participation of Fe(H_2O_2) in substrate oxidation, since the uncoupling process is reversible, whereas the O−O bond homolysis leads irreversibly to substrate oxidation. This will increase the fraction of oxidation by Fe(H_2O_2), but we cannot determine to what extent. Further increase in the amount of substrate oxidation by Fe(H_2O_2) can be anticipated if it can undergo fast deprotonation and be converted to Cpd 0 at the expense of uncoupling and production of free H_2O_2.

The KIE and [**2**/**3**] ratio are good probes for distinguishing between the reactivity of Cpd I and Cpd 0 or Fe(H_2O_2). Thus, Cpd I will give rise to large KIE values (7 or so) and high [**2**/**3**] ratio, while the other two reagents will give rise to small KIE values (2 or so) and inverse [**2**/**3**] ratios. Another probe for the reactivity of Cpd I is the previously predicted[24,25d] product kinetic isotope effect on the ratio [**2**/**3**]. The predicted product isotope effect arises from the fact that the processes which lead to **2** and **3** arise from the two spin states of Cpd I and possess different KIE values; **2** is generated mostly (or only) from the reactivity of the low-spin state of Cpd I, while **3** is generated exclusively from the high-spin state.

Conclusions

The DFT study of C−H hydroxylation by the Cpd I, Cpd 0, and Fe(H_2O_2) species of P450 (Scheme 1) reveals the following trends:

The high-valent oxo-iron Cpd I species is the most reactive among the three species. When Cpd I is present, the other two reagents will be silent. Thus, C−H hydroxylation by the wild-type enzyme will proceed via the classical "rebound mechanism",[9] with two reactive states (TSR)[24,25] of Cpd I leading to products

In the absence of Cpd I, we may anticipate substrate oxidation by Cpd 0 and Fe(H_2O_2) through a stepwise mechanism that involves initial O−O bond homolysis followed by H-abstraction

from the substrate. These reactions will be sluggish compared with oxidation by Cpd I.

Cpd 0 is expected to undergo 85% of porphyrin hydroxylation vis-à-vis only 15% of substrate oxidation. The substrate oxidation will lead mostly to the rearranged alcohol, **3** (Scheme 2).

Fe(H_2O_2) is expected to undergo mostly uncoupling and produce free hydrogen peroxide. A small fraction of the reagent will carry however substrate oxidation and lead mostly to the rearranged alcohol, **3**.

The kinetic isotope effect (KIE) for substrate oxidation by Cpd 0 or Fe(H_2O_2) will be small, ~2,[18a] while that by Cpd I will lead to a significant KIE.[9,24,37] Furthermore, the KIE values for the generation of for **2** and **3** via Cpd I will be different, leading to a product isotope effect.[24]

Typically both Cpd 0 and Fe(H_2O_2) will lead to a very small **2**/**3** ratio of the products, while Cpd I will lead to high ratios.

One question remains and should be answered by experiment: *Is Cpd I really absent in the proton-relay mutants of P450 (e.g., T252A)*?[2] If the answer to this question is positive, then our study provides probes for the reactivity of Cpd 0 and Fe(H_2O_2). As such, this detailed study can form a basis for interplay between experiment and theory.

Acknowledgment. The research was supported by a grant from BMBF-DIP (Grant No. DIP-G.7.1). S.S. is thankful to J. P. Dinnocenzo for illuminating discussions.

Supporting Information Available: Tables (33), figures (10), and *xyz* coordinates of all calculated species (PDF). This material is available free of charge via the Internet at http://pubs.acs.org.

JA056328F